

## Plasma Density Control by Molecular Beam Injection in HT-7 Tokamak

WU Yingxiang<sup>1</sup>, LI Jiangang<sup>2</sup>, WAN Baonian<sup>2</sup>, GONG Xianzu<sup>2</sup>, GU Xuemao<sup>2</sup>,  
LUO Jiarong<sup>2</sup>, WANG Xiaoming<sup>2</sup> and MORITA Shigeru<sup>3</sup>

<sup>1</sup>*Institute of Mechanics, Chinese Academy of Science, Beijing, China*

<sup>2</sup>*Institute of Plasma Physics, Chinese Academy of Science, Hefei, China*

<sup>3</sup>*National Institute for Fusion Sciences, Toki, Japan*

(Received: 9 December 1998 / Accepted: 3 September 1999)

### Abstract

Laval nozzle, which produces supersonic molecular beam, is proven to be an effective fuelling tool for magnetic confinement devices. Details of its design are given in the first part of this paper. Results with supersonic beam injection in HT-7 tokamak show higher efficiency and deeper penetration compared to normal gas puffing. The peaking factor is almost the same with the off-axis pellet injection. Experiments demonstrate that it is a suitable fuelling method of steady-state operation with high density for super-conducting tokamak.

### Keywords:

HT-7, Laval nozzle, supersonic molecular beam, gas puffing

### 1. Introduction

To fuel tokamak plasma in more efficient way is very important issue for fusion research. Pellet injection is proven to be very effective, but it is difficult for steady-state operation. Normal gas puffing is not proper for reactor relevant performance due to its fuelling efficiency and recycling problem. Oriented supersonic molecular beam injection may be a good candidate for fuelling in steady-state operation with high density. The molecular beam was successfully injected to the HL-1M tokamak and proven that it is more effective than the normal gas puffing [1-2]. According to aerodynamic principle, Laval nozzle is the key device to produce supersonic molecular beam [3]. HT-7 is a super-conducting tokamak emphasized on high performance steady-state operation. For getting steady-state high-density plasma, a Laval nozzle was designed and installed in the HT-7 tokamak. Its experiments were carried out in the HT-7 tokamak. The main purpose of

the experiments is to optimize its parameter for the high-density steady-state fueling, deeper penetration and reduce the high edge recycling made by strong gas puffing. The detail of the Laval nozzle design was described in the first part of the paper. The experimental results were given in the following part.

### 2. Gas Injector Design

As we know, in order to obtain a supersonic, parallel, uniform molecular beam at the exit section of an injector, a Laval-shaped nozzle must be used to achieve this goal. The gas in a Laval nozzle will flow from subsonic (convergent section) through transonic (throat section) to supersonic (divergent section) shown in Fig. 1. Owing to the different flow properties in each flow section, the design method should be different.

---

Corresponding author's e-mail: yxwu@imech.ac.cn

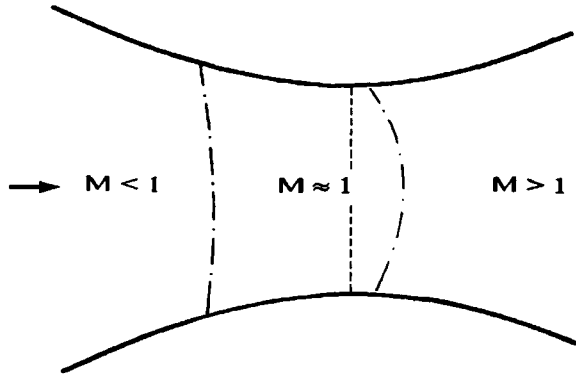


Fig. 1 Flow property in a Laval Nozzle.

**2.1 The design of a Laval nozzle transonic section**

According to aerodynamic theory, if the flow at the throat of a nozzle reaches maximum discharge, the flow in divergent section of the nozzle will be supersonic, and in supersonic area, the downstream flow will have no influence on upstream flow. Therefore, we can deal with the flow in subsonic area and transonic area separately.

The flow parameters in transonic area can be solved by the method created by Lin and Jia [4] who used a stream function to govern the flow field:

$$\psi(\xi, \eta) = 2 \left( \frac{\gamma + 1}{2} \right)^{\frac{1}{\gamma - 1}} g(\xi) \int_0^\eta \left[ 1 - \frac{\gamma - 1}{\gamma + 1} \frac{g^2(\xi)}{H_1^2(\xi, \eta)} \right]^{\frac{1}{\gamma - 1}} \frac{H_2(\xi, \eta)}{H_1(\xi, \eta)} y(\xi, \eta) d\eta,$$

where  $H_1(\xi, \eta)$  and  $H_2(\xi, \eta)$  are the inverse of the Lamé coefficients for the transformation between the orthogonal curvilinear coordinates  $(\xi, \eta, \theta)$  and the orthogonal curvilinear coordinates  $(x, y, \theta)$ ;  $\gamma$  is the specific heat ratio;  $g(\xi)$  is rather complex, we do not describe it here. The reader who is interesting in it can refer to reference [4].

For simplicity, we choose a circular type wall as the throat section of the Laval nozzle, so the employment of double circular coordinates will be convenient. The coordinates and the Lamé coefficient for this conformal curvilinear coordinate transformation are as follow:

$$x = \frac{\coth(\eta_b) \sinh(2\xi)}{\cosh(2\eta) + \cos(2\xi)}, \quad y = \frac{\coth(\eta_b) \sin(2\eta)}{\cosh(2\eta) + \cos(2\xi)},$$

$$H_1(\xi, \eta) = \frac{2 \coth(\eta_b)}{\cosh(2\eta) + \cos(2\xi)},$$

$$H_2(\xi, \eta) = \frac{2}{\sinh(2\eta)}.$$

The constant  $\eta_b$ , which is chosen to make the throat radius being 1, is computed by

$$\eta_b = \cos^{-1}(\sqrt{2r}).$$

Here  $r$  is the throat radius. Substituting the expressions of  $y, H_1, H_2$  into the equation of  $\Psi$ , and with the maximum discharge condition at the throat section, we can obtain the stream function  $\Psi$ , then we can obtain the velocity, pressure, density and temperature in the flow field by:

$$q^2 = u^2 + v^2, \quad u = \frac{\Psi_\eta}{\rho y H_2}, \quad v = -\frac{\Psi_\xi}{\rho y H_1},$$

$$\rho = \left( \frac{\gamma + 1}{2} - \frac{\gamma - 1}{2} q^2 \right)^{\frac{1}{\gamma - 1}}, \quad T = \frac{\gamma + 1}{2} - \frac{\gamma - 1}{2} q^2,$$

$$p = \left( \frac{\gamma + 1}{2} - \frac{\gamma - 1}{2} q^2 \right)^{\frac{\gamma}{\gamma - 1}}.$$

**2.2 The design of a Laval nozzle in supersonic section**

In order to obtain the flow parameters and the wall shape of a Laval nozzle in supersonic area, we had better use characteristic method. The basic equations to govern the flow-field are:

$$\frac{dq}{q} d\theta \cdot \tan(\mu) \mp \frac{\sin(\theta) \cdot \sin(\mu) \tan(\mu)}{\cos(\theta \pm \mu)} \frac{dx}{y} = 0,$$

$$\left( \frac{dy}{dx} \right)_{1,2} = \tan(\theta \pm \mu).$$

Here  $q$  is the velocity in the flow-field,  $\theta$  is the flow direction, and  $\mu$  is the Mach angle defined by

$$\mu = \sin^{-1} \frac{1}{M}.$$

$M$  is the local Mach number in the flow field.

In order to obtain the parallel gas flow at the exit section of the Laval nozzle, there must be no reflection wave from the wall of the nozzle into the inner flow field of the nozzle. To realize this, when the expansion

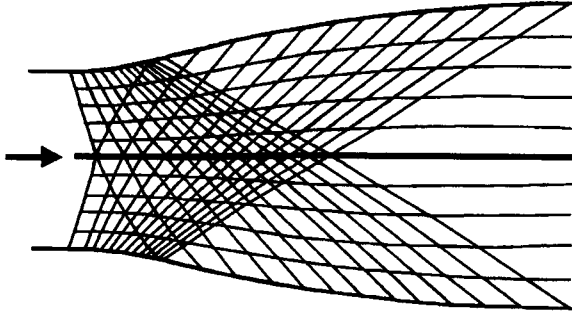


Fig. 2 Design of an ideal gas injector in supersonic region.

waves reach the wall, they must be absorbed totally by the wall. By this condition, we can obtain the shape of the nozzle step by step with characteristic equations until the flow parameters at the exit section of the nozzle are parallel and uniform. In this way, the supersonic section of the Laval nozzle can be designed (see Fig. 2).

### 2.3 The design of a Laval nozzle in subsonic section

The design of a Laval nozzle in subsonic section is very simple, as we can use one-dimensional flow theory to treat it. The relation between section areas and Mach numbers is:

$$\frac{A_1}{A_2} = \frac{M_2}{M_1} \left( \frac{1 + \frac{\gamma-1}{2} M_1^2}{1 + \frac{\gamma-1}{2} M_2^2} \right)^{\frac{\gamma+1}{2(\gamma-1)}}$$

By using the Mach number next to the transonic area and adjusting the Mach number at each section, we can obtain the shape of the nozzle in subsonic section. In this way, we designed a helium gas injector with 1 mm in diameter at throat section and 6mm in diameter at and exit section that can produce parallel and uniform gas beam at about 2200m/s at exit section of the injector. For deuterium working gas, the speed at the exit section is about 3.2km/s.

## 3. Experimental Results

Supersonic beam has been proven to be a very effective fuelling method in HT-7 tokamak. Typical results were shown in Fig. 3. The valve was switched on at 200ms and lasted for 10ms. Central chord line averaged electron density raised quickly and kept increasing from  $1 \times 10^{13} \text{cm}^{-3}$  to  $4 \times 10^{13} \text{cm}^{-3}$  in 250ms

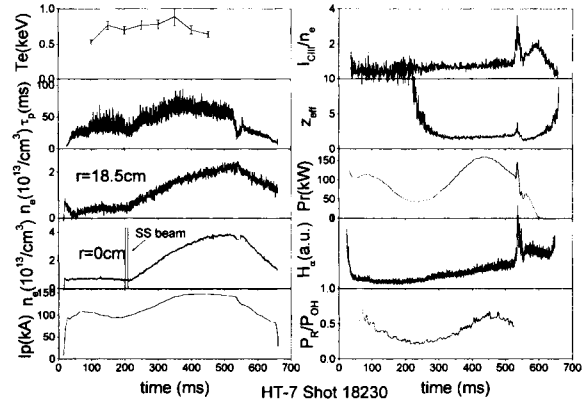


Fig. 3 Typical results in supersonic gas puffing at 200ms for 10ms.  $B_T = 1.8T$ .

after switching on the beam. Chord averaged electron density at 18.5cm increased too. But its rate was lower than that at central chord, implying more peaked electron density profile.  $H_\alpha$  emission increased slightly with the increasing of electron density, which means that supersonic beam puffing does not cause serious recycling comparing with strong gas puffing case. However global particle confinement was improved considerably.  $Z_{\text{eff}}$  decreased to 2 after supersonic beam was puffed. The ratio of CIII emission intensity to electron density implied that supersonic beam puffing did not bring any impurity problem. Radiation power and ratio of radiation power to ohmic power increased with increasing of electron density. Measurement by SX PHA showed a slight electron temperature variation after supersonic beam was puffed. The stored energy in plasma was increased after supersonic beam injection. This might be an effect of improved global confinement and decreased impurity contents.

As comparison with supersonic gas puffing, Fig. 4 showed a typical result for normal gas puffing at 140ms lasting for 150ms duration. To keep electron density increasing, gas puffing must be applied for a much longer duration compared to supersonic gas puffing. Similar plasma performance was obtained. However, radiation power increased strongly with increasing of electron density due to little variation in  $Z_{\text{eff}}$ . Increasing rate of electron density at central chord and chord at 18.5cm are nearly same that implied little change in electron density profile during gas puffing. To compare the delayed time of electron density after two different gas puffing and electron density profile, we show the ratio of electron densities from central chord to the

chord at 18.5cm shown in Fig. 5. Clearly, electron density started to increase in supersonic gas puffing

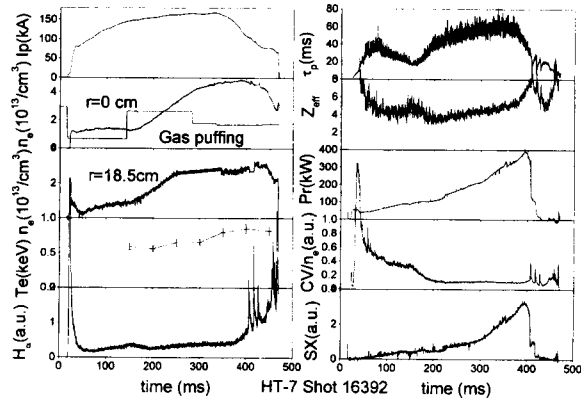


Fig. 4 Typical results for normal gas puffing.

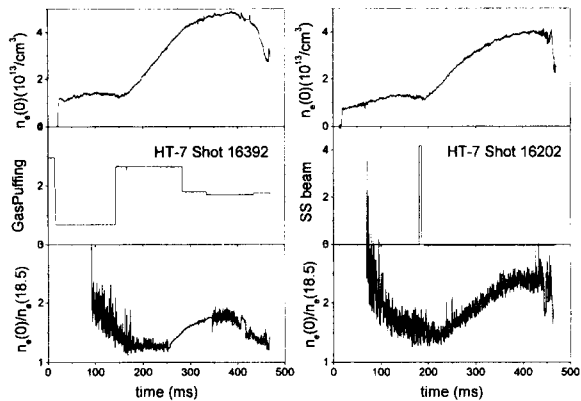


Fig. 5 Comparison of performance in electron density with supersonic and normal gas puffing.

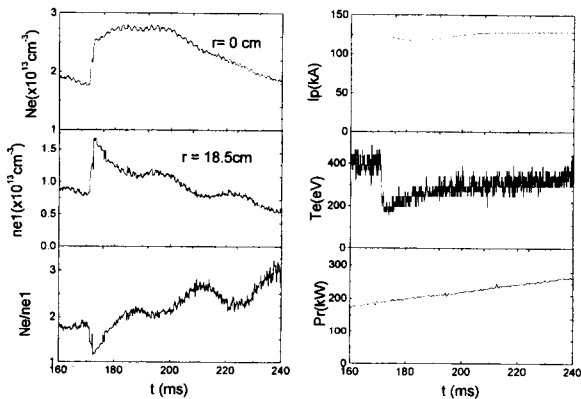


Fig. 6 Off-axis pellet injection shot for compare with supersonic gas injection.  $B_T = 1.8T$ .

more quickly than that in normal gas puffing. Also electron density profile after supersonic gas puffing became more peaked.

As comparison with pellet injection, an off-axis pellet injection shot was shown as Fig. 6. The pellet was injected to the radius  $r = 11\text{cm}$ , which was nearly the same penetration depth with supersonic beam. The pellet was fired at 172ms. The plasma density at chord 18.5cm raised immediately and followed the increase of density in the center. The ration of  $n_e(0)/n_e(18.5)$  dropped in the first few milliseconds that implied the density profile became flatten. The density profile became peaked within 10ms and reached its highest value in 30ms, which was close to the particle confinement time. The central electron temperature dropped from 400eV to 200eV after pellet injection and gradually recovered. The radiation power increased slowly with the time and showed a different pattern with the density as the case of gas puffing. Since there was only three channels for HCN interferometer, it was very difficult to get accurate peaking factor measurement. Here, the ratio of  $n_e(0)/n_e(18.5)$  was used as quantitative factor to compare the density peaking during normal gas puffing, supersonic beam and pellet injection. The ratio is 1.5 for the gas puffing, 2.4 for supersonic beam and 2.6 for the off-axis pellet injection. For on-axis pellet injection, this ratio is about 3.1 that implied more peaked density profile. For the off-axis fueling, the pellet didn't show it advantage to supersonic beam since the peaking factor was almost same. But for the particle-fueling rate for pellet injection, it showed higher than 87%. The particle fueling rates for supersonic injection and normal gas puffing were 65% and 30% respectively. On the other hand, the multi-pellet injection for the stable density fueling under steady state condition is very difficult at moment.

To monitor penetration of supersonic beam into plasma, A photo diode array was installed in the bottom window of the same port of Laval nozzle to observe  $H_\alpha$  line emission. Results were shown in Fig. 7. The spatial resolution of the array was 1.7cm. Results showed that a mount of supersonic beam could penetrate nearly up to plasma center for this special case, while the beam only penetrated to a depth of 12~15cm inside of plasma for normal condition. The penetration depth observed was more than prediction by Monte-Carlo code, which predicted penetration of 15cm inside of plasma ( $r = 12\text{cm}$ ) in present HT-7 target plasma. This discrepancy might be caused by neglecting the molecular processes and steady-state assumption in simulation. The beam

should penetrate more if ionization and dissociation of molecules are considered. In principle, assumption of steady state is not true because the cold channel formed around beam is beneficial for penetration of next coming neutral particles. More detail work about this will be carried out on HT-7 in near future.

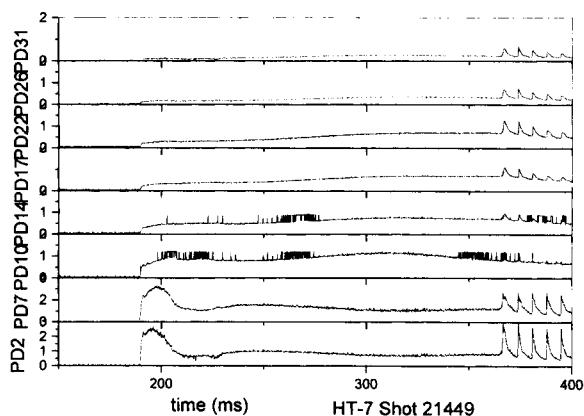


Fig. 7  $H_\alpha$  photo diode array monitoring the penetration of supersonic beam.

#### 4. Conclusion

To get steady-state high-density plasma, the Laval nozzle has been installed in the HT-7 superconducting tokamak and experiments have been carried out. The high-density plasma could easily be controlled by pulsed high-speed molecular beam that comes from the Laval nozzle. The speed of the hydrogen beam is about 1.5~2.8km/s that mainly depends on the temperature of the injection gas and the plasma condition. With penetration depth up to plasma center, the density peaking factor is almost the same with the one achieved by off-axis pellet injection. The improvements for both energy and particle confinements were achieved by molecular beam injection. Fueling efficiency of about 65% demonstrates that it is a useful tool for the steady-state tokamak operation.

#### References

- [1] L.H. Yao *et al.*, Nucl. Fusion **38**, 736 (1998).
- [2] L.H. Yao *et al.*, 17th IAEA Fusion Energy Conference, Yokohama, Japan, Oct. 1998, IAEA-CN-60/FTP/25.
- [3] G. Scoles, *Atomic and Molecular Beam Methods* Vol. **1**, (New York, Oxford, Oxford Press, 1998) P.15.
- [4] T.J. Lin and Z.X. Jia, *Proc. Indian Academy of Sci.* Vol. **4**, Part 3, 315 (1983).